Journal of Biomolecular NMR **29:** 319–324, 2004.

Adiabatic heteronuclear decoupling in rotating solids

Jörg Leppert, Oliver Ohlenschläger, Matthias Görlach & Ramadurai Ramachandran*
Abteilung Molekulare Biophysik/NMR-Spektroskopie, Institut für Molekulare Biotechnologie, 07745 Jena, Germany

Received 11 December 2003; Accepted 15 March 2004

Abstract

In magic angle spinning solid state NMR experiments the potential of heteronuclear ^{1}H decoupling employing a continuous train of adiabatic inversion pulses has been assessed via numerical simulations and experimental measurements. It is shown that, with a ^{1}H RF field strength of $\sim$ 100 kHz that is typically available in MAS NMR probes, it is possible to achieve efficient adiabatic ^{1}H decoupling at low magic angle spinning frequencies. It is pointed out that in the presence of H_1 inhomogeneities it will be advantageous to employ adiabatic decoupling in MAS solid state NMR experiments.

Introduction

Heteronuclear decoupling is routinely employed both in solution and solid state NMR investigations for enhancing signal intensities and for improving spectral resolution (Ernst et al., 1987; Schmidt-Rohr and Spiess, 1994). In liquid state NMR studies of isotopically labelled biological systems ^{1}H nuclei are typically observed and scalar coupling interactions with ^{15}N and ^{13}C nuclei are simultaneously eliminated via suitable RF irradiation of the heteronuclei. In solids, low γ heteronuclei are generally observed with simultaneous irradiation on the ^{1}H nuclei to eliminate scalar and dipolar interactions with the abundant spins. Several decoupling schemes have been reported in the literature for liquid state NMR applications. These involve typically the application of composite or adiabatic inversion pulses with suitable phase cycles and supercycles (Levitt et al., 1983; Shaka and Keeler, 1987; Kupce and Freeman, 1995, 1996). Heteronuclear decoupling in solids was initially achieved by continuous wave (CW) high power RF irradiation of the ^{1}H nuclei. However, a variety of decoupling schemes for solid state NMR applications have also been reported (Bennett et al., 1995; Eden and Levitt, 1999; Gan and Ernst, 1997; Ernst, 2003; Ernst et al., 2003; De Paëpe et al., 2003; Gerbaud et al., 2003). The two pulse phase modulation (TPPM) decoupling scheme of Bennett et al. (1995) is currently extensively used in the literature. It consists of two pulses each with a flip angle of about 180° and a phase difference between the pulses on the order of 10°–50° and provides superior performance relative to CW decoupling. The performance characteristics of the TPPM decoupling scheme is sensitive to the precise values of the pulse length and phase angles employed. The optimal values for these parameters depend on the MAS frequency, RF-field strength etc.. The X-inverse-X (XiX) decoupling scheme (Detken et al., 2002) involving the repeated application of two pulses of equal length with a phase difference of 180° overcomes some of the limitations of TPPM. Unlike TPPM, obtaining the best XiX decoupling performance requires only the optimisation of a single parameter value, namely the pulse length. The relative merits of XiX and TPPM decoupling schemes have been discussed recently (Ernst, 2003a) and at very high MAS frequencies and at high RF-field strengths the decoupling performance of the XiX scheme is found to be better than TPPM. The XiX sequence is also less sensitive to RF-field inhomogeneities than the TPPM decoupling sequence (Detken et al., 2002).

Although studies at very high spinning frequencies are very attractive, often it may be necessary or sufficient to carry out MAS NMR experiments at low spinning speeds. For example, experiments

*To whom correspondence should be addressed. E-mail: raman@imb-jena.de

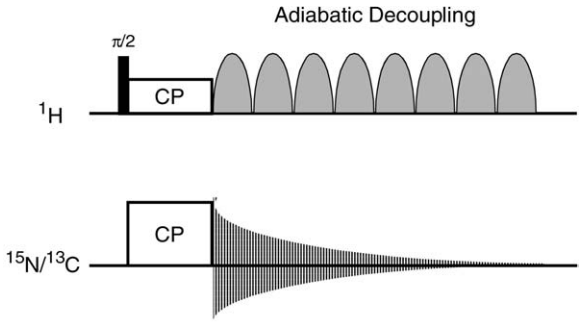

Figure 1. CPMAS pulse sequence with adiabatic decoupling sequence applied on the ^{1}H channel. The adiabatic inversion pulses were phase cycled as described in the text.

that require the analysis of the intensities of a sufficient number of spinning sidebands for obtaining information about torsion angles (Hong et al., 1997, 1998), internuclear distances (DiVerdi and Opella, 1982; Roberts et al., 1987) and CS tensor principal values and orientations (Goetz et al., 1997; Leppert et al., 2000a, b, 2001; Heise et al., 2001; O'Connor et al., 2002) necessarily have to be carried out at low spinning speeds. With many biological systems it may also be difficult to employ very high spinning speeds, for example to avoid sample dehydration. Even in situations where the spinning sidebands are not required, moderate MAS frequencies may be sufficient in studies involving nuclei such as ^{15}N. Experiments such as REDOR (Gullion and Schaefer, 1989) are often carried out at low MAS frequencies to minimise cumulative signal losses arising out of imperfect inversion pulses employed. Hence, it will be advantageous for applications at low MAS frequencies to have a decoupling scheme that is easy to implement, performs as good as or better than TPPM and is not affected by nonideal experimental conditions such as the presence of RF field inhomogeneities. Therefore, we have examined the potential utility of adiabatic heteronuclear decoupling in rotating solids. The motivation for this work comes from the excellent performance seen with adiabatic decoupling sequences in liquid state NMR (Kupce and Freeman, 1995, 1996) and from our recent studies (Leppert et al., 2002, 2003; Heise et al., 2002) where adiabatic inversion pulses were successfully employed in MAS NMR experiments such as REDOR and RFDR to overcome H_1 inhomogeneity and resonance offset effects.

Numerical and experimental procedures

A critical factor that determines the adiabatic pulse width in liquid state decoupling schemes is to have a large decoupling bandwidth at low RF power levels, because an average RF power dissipation on the order of 1–2 Watts is typically allowed by liquid state probe specifications. Hence, adiabatic inversion pulses used in liquid state decoupling applications have large durations on the order of ∼1 ms. The small magnitude of heteronuclear scalar couplings permits the usage of long adiabatic pulses in liquid state decoupling sequences (Kupce and Freeman, 1995, 1996). However, the presence of much larger heteronuclear dipolar couplings precludes the usage of such long inversion pulses in the solid state. On the other hand, a decoupling RF field strength on the order of ∼100 kHz is typically employed in solid state NMR studies. The availability of such high power RF handling capabilities in solid state NMR experiments permits the usage of short inversion pulses in decoupling sequences and such sequences can be effectively employed at low MAS frequencies as shown below.

We have employed the tanh/tan adiabatic inversion pulse (Hwang et al., 1998) constructed from the following adiabatic half passage and its time reversed half passage:

$$\omega_1(t) = \omega_1(\mathrm{max}) \tanh[\xi 2t/T_p], \quad (1)$$

$$\Delta\omega(t) = \Delta\omega_{\mathrm{max}}[\tan(\kappa(1 - 2t/T_p))]/\tan(\kappa), \quad (2)$$

where $\xi = 10$, $\tan(\kappa) = 20$ and $0 \leq t \leq T_{\mathrm{p}}/2$. The frequency sweep is implemented in the spectrometer hardware as a phase modulation, $\phi(t) = \int \Delta\omega(t)dt$. A value of 60 was employed for the parameter R, representing the product of the adiabatic pulse bandwidth and the pulse length (Hwang et al., 1998). Far off resonance, the tanh/tan adiabatic pulse employs very fast frequency sweeps and at the two extremities of the sweep the amplitude is brought down smoothly to zero. In assessing the efficacy of heteronuclear decoupling with a continuous train of adiabatic inversion pulses we considered phasing schemes such as (p5)(m4) and (p5)(p7)(m4) where p5, p7 and m4 represent the phase cycles {0°, 240°, 240°, 60°, 0°}, {0°, 105°, 300°, 255°, 300°, 105°, 0°} and {0°, 0°, 180°, 180°}, respectively (Tycko et al., 1985; Levitt et al., 1983; Leppert et al., 2003). Numerical simulations were performed using the SIMPSON program (Bak et al., 2000) with a Zeeman field strength of 11.7 T, typical ^{15}N and ^{13}C dipolar coupling parameters and

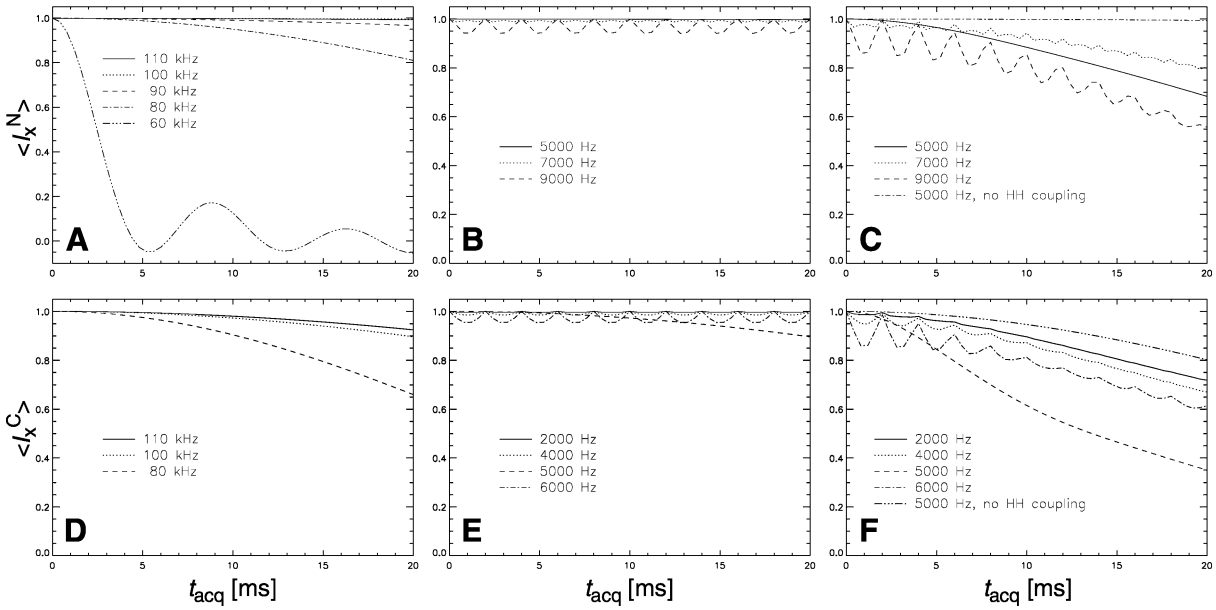

Figure 2. Simulations of the free induction decays in the NH (A, B), NH_2 (C), CH (D,E) and CH_2 (F) spin systems. (A) and (D) show the dependence on the decoupler RF field strength at a spinning speed of 5 kHz. The plots in Figures 2B, 2C, 2E and 2F were obtained with a RF field strength of 100 kHz at the spinning speeds indicated. Adiabatic decoupling was achieved using the tanh/tan pulses with the (p5)(m4) phasing scheme. The dipolar coupling strengths employed in these simulations were $D_{NH} = 9.3$ kHz, $D_{CH} = 23.3$ kHz and $D_{HH} = 21.2$ kHz. The time domain data were sampled in steps of 400 μs. Heteronuclei were kept on resonance and CSAs were neglected.

spinning speeds as indicated in the figure captions. Experiments were carried out either with an undiluted ^{15}N,^{13}C labelled sample of histidine at room temperature or with an ^{15}N labelled RNA sample (see below) on a 500 MHz wide bore Varian ^{UNITY}*INOVA* solid state NMR spectrometer equipped with a 5 mm DOTY supersonic triple resonance probe and a waveform generator for pulse shaping. Cross-polarisation under Hartmann-Hahn matching conditions was employed and all spectra, unless mentioned otherwise, were collected employing the RF pulse sequence shown in Figure 1. Other details are given in the figure captions.

Results and discussion

Considering heteronuclear two and three spin networks of the type XH/XH2, the evolution of the transverse X spin magnetisation (X_X) under the RF irradiation applied to the ^1H spin was monitored without assuming any synchronous relationship between the decoupling sequence and the rotor period. In the studies reported here an RF field strength on the order of 100 kHz was considered as this corresponds to the situation with our experimental set up. Under this condition it was observed from numerical simulations and experimental measurements (see below) that tanh/tan adiabatic pulses with a duration of 20 μs can provide satisfactory decoupling performance at low MAS frequencies. The simulated FID trajectories under adiabatic heteronuclear decoupling are shown in Figure 2. These plots were generated neglecting the X spin CSA and by keeping the X spin on resonance. Under this condition perfect decoupling corresponds to $< X_X(t) >= 1$ at all times (Bennett et al., 1995), i.e., when there are no large variations or oscillations in the amplitude of the transverse magnetisation. It was seen that differing phasing schemes mentioned earlier lead to equally efficient ^1H decoupling (data not shown). All the simulated FID trajectories shown in Figure 2 were generated with the (p5)(m4) scheme. At low spinning speeds, as seen from the plots in Figure 2A, an efficient adiabatic ^1H decoupling employing an RF field strength of ∼100 kHz can be obtained. Figure 2B shows the FID generated in a NH spin system as a function of the spinning speed employed. The data for spinning speeds less than 5 kHz are found to be similar to that shown for 5 kHz. The oscillations in the FID seen at 9 kHz indicate that degradation in the decoupling performance begins to appear only at high MAS frequencies. The plots in Figure 2C were generated as a function of the spinning speed with a

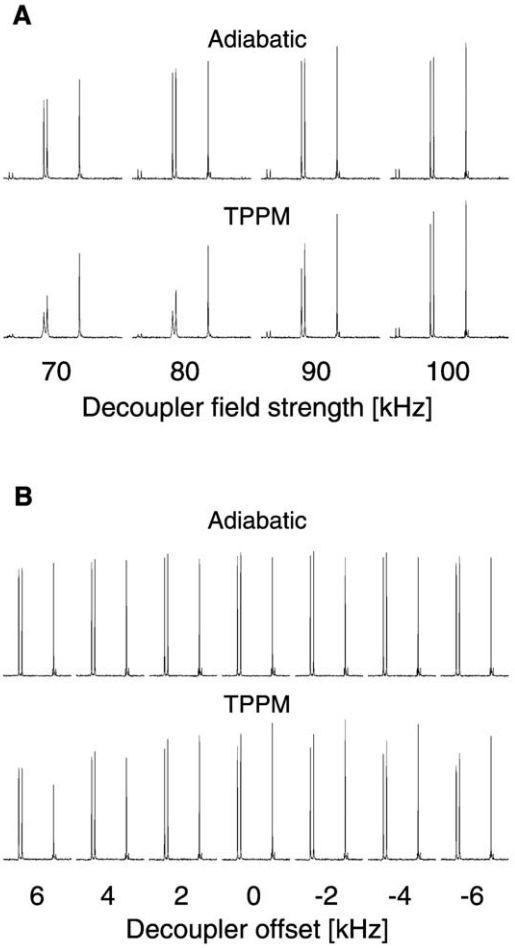

Figure 3. ^{15}N CPMAS spectra of histidine obtained at a spinning speed of 7 kHz employing a data acquisition time of 20 ms with a CP contact time of 1 ms. The spectra were collected, employing adiabatic and TPPM decoupling schemes, as a function of the decoupler RF field strength (A) and decoupler offset (B). With a recycle time of 10 s, 16 transients were collected. Spectra shown in figure B were collected with a ^{1}H RF field strength of ∼100 kHz. Adiabatic decoupling was achieved employing the tanh/tan pulses with (p5)(m4) phasing scheme. TPPM decoupling scheme consisted of two pulses each with a flip angle of 5.1 μs and a phase difference of 40° between the pulses.

decoupling RF field strength of 100 kHz, considering a NH_2 spin system and including the proton-proton dipolar interaction in the simulation. Figure 2C also shows for comparison the FID generated at 5 kHz neglecting the homonuclear dipolar interaction. The presence of strong homonuclear dipolar coupling in a XH2 spin system makes ^{1}H decoupling generally more difficult compared to the XH case (Bennett et al., 1995; Ernst, 2003; Ernst et al., 2003). The performance of adiabatic decoupling in the XH2 case, with protons dipolar coupled to either ^{15}N or ^{13}C, is also not as efficient as for the simple XH spin system. Representative simulated FIDs corresponding to the CH and CH2 cases are given Figures 2D–2F. Figure 2D and 2E show the decoupling performance as a function of the RF field strength and spinning speed employed. The plots shown in Figure 2D were obtained at a spinning speed of 5 kHz and the plots in Figure 2E were generated employing a RF field strength of 100 kHz. Figure 2F shows the simulated FIDs for the CH2 case as a function of the spinning speed. As in the NH case a RF field strength of ∼100 kHz can provide satisfactory decoupling performance also in ^{13}C NMR investigations (Figure 2D). However, due to the larger magnitude of the ^{13}C–^{1}H dipolar coupling strength relative to that of the ^{15}N–^{1}H dipolar coupling, the adiabatic decoupling performance seen for the NH and NH2 spin systems is better than that observed for the CH and CH2 cases.

We have also assessed experimentally the performance of the adiabatic decoupling scheme. These results are in agreement with the numerical simulations. Figures 3–6 show a few representative experimental results. Figures 3A and 3B, respectively, show at a spinning speed of 7 kHz, the decoupler RF field strength and offset dependence of the signal intensity in the ^{15}N spectrum of histidine. For comparison the corresponding spectra obtained with TPPM decoupling are also given. In agreement with numerical simulations, the performance of the adiabatic decoupling sequence is seen to be less sensitive to the RF field strength. Adiabatic decoupling also shows (Figure 3B) satisfactory performance over a range of ^{1}H resonance offsets. From these results one can conclude that under non-ideal conditions, e.g. in the presence of H_1 inhomogeneity, it may be advantageous to employ adiabatic decoupling in ^{15}N MAS NMR studies. ^{15}N MAS NMR is expected to play a critical role in the structural studies of RNAs via solid state NMR. Figure 4 shows the ^{15}N CPMAS NMR spectra of an 100 kDa RNA sample containing 97 CUG triplets representing the CUG triplet expansion repeat of the 3′–nontranslated region of DM protein kinase (Brook et al., 1992), that is currently under investigation in our laboratory. These spectra were collected employing different decoupling schemes. The superior performance of adiabatic and TPPM decoupling relative to that of CW decoupling is evident. In this study the sample volume was restricted essentially to the central portion of the rotor. As H_1 inhomogeneity effects are expected to be minimal, the performance of TPPM is

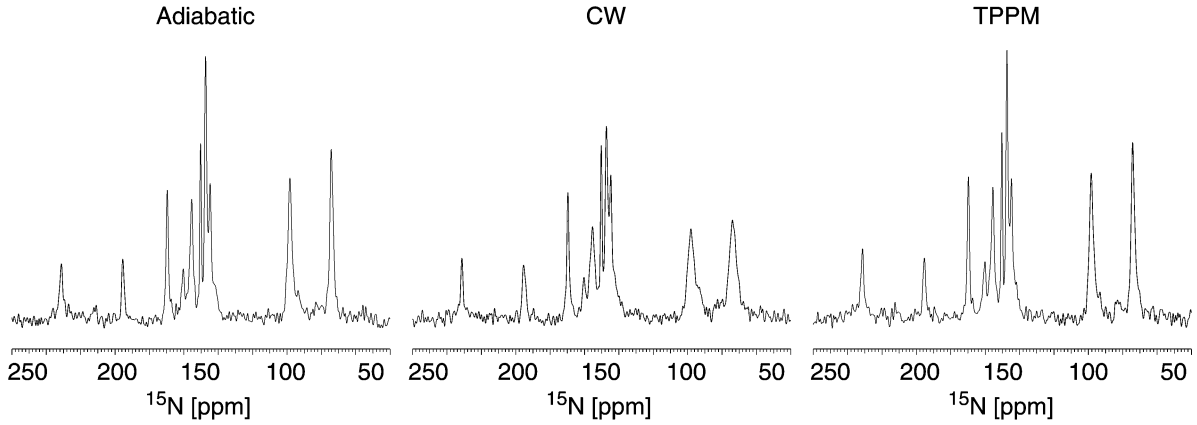

Figure 4. ^{15}N CPMAS spectrum of the hydrated $(CUG)_{97}$ RNA sample obtained at a spinning speed of 7 kHz and a temperature of $\sim -15\,^{\circ}$C employing a data acquisition time of 20 ms with a CP contact time of 2 ms, a recycle time of 10 sec and 1024 transients. Spectra were collected employing the decoupling schemes indicated and with a ^{1}H RF field strength of $\sim$100 kHz. The chemical shifts are referenced to external $^{15}NH_4Cl$ ($\delta_N = 38.5$ ppm).

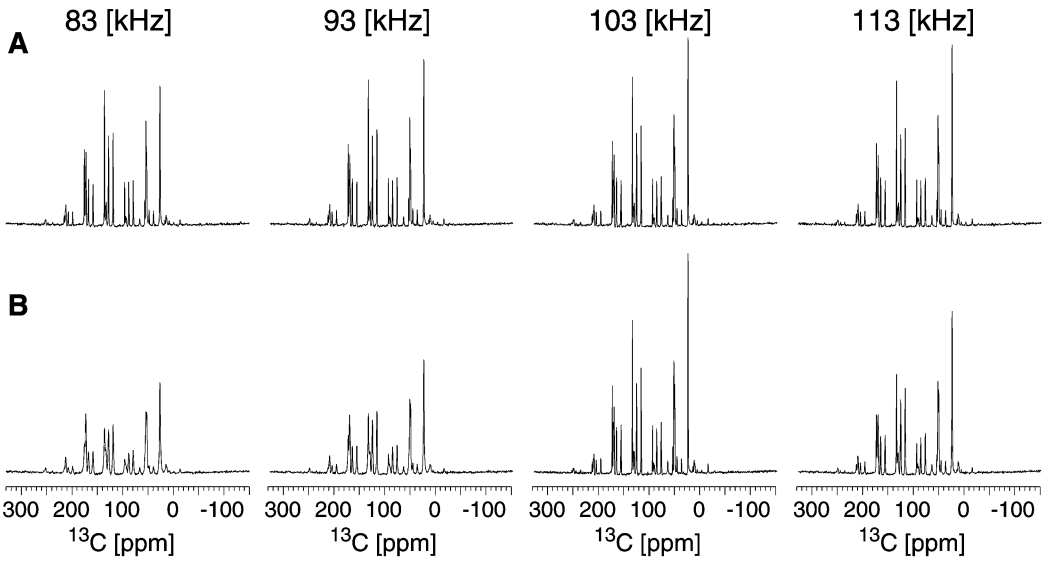

Figure 5. ^{13}C CPMAS spectra of histidine obtained at a spinning speed of 5 kHz employing a data acquisition time of 15 ms with a CP contact time of 2 ms. The spectra were collected as a function of the decoupler RF field strength indicated, employing (A) adiabatic and (B) TPPM decoupling schemes. 4 transients were collected with a recycle time of 20 sec. Tanh/tan pulses with the (p5)(m4) phasing scheme were used for the adiabatic decoupling scheme. TPPM decoupling scheme consisted of two pulses each with a flip angle of 5.1 μs and a phase difference of 40° between the pulses. The spectra were indirectly referenced to external adamantane ($\delta_{CH} = 29.5$ ppm with respect to TMS).

comparable to that of the adiabatic decoupling. Figure 5 shows at a spinning speed of 5 kHz the RF field strength dependence of the signal intensity in the ^{13}C spectrum of histidine acquired under adiabatic and TPPM decoupling schemes. At the spinning speed employed the decoupling of the methylene carbon at 26 ppm is achieved better by TPPM. However, unlike TPPM, the performance of adiabatic decoupling is not very sensitive to the precise setting of the RF field strength employed. In conclusion, the results presented in this work suggest that in NMR studies carried out at low MAS frequencies, it is possible to achieve satisfactory heteronuclear decoupling employing a RF field strength on the order of $\sim$ 100 kHz. Adiabatic de-

coupling is easy to implement and is a robust scheme that is tolerant to H_1 inhomogeneity and ^{1}H resonance offsets. If higher decoupling RF field strengths are available it may also be possible to extend the applicability of the adiabatic decoupling scheme to higher MAS frequencies. As the adiabatic decoupling scheme is effective at low MAS frequencies, it is expected that even in static solid state NMR experiments it will be equally effective.

References

Bak, M., Rasmussen, J.T. and Nielsen, N.C. (2000) *J. Magn. Reson.*, **147**, 296–330.

Bennett, A.E., Rienstra, C.M., Auger, M., Lakshmi, K.V. and Griffin, R.G. (1995) *J. Chem. Phys.*, **103**, 6951–6958.

Brook, J.D., McCurrach, M.E., Harley, H.G., Buckler, A.J., Church, D., Aburatani, H., Hunter, K., Stanton, V.P., Thirion, J.P., Hudson, T. et al. (1992) *Cell*, **68**, 799–808.

De Paëpe, G., Hodgkinson, P. and Emsley, L. (2003) *Chem. Phys. Lett.*, **376**, 259–267.

Detken, A., Hardy, E.H., Ernst, M. and Meier, B.H. (2002) *Chem. Phys. Lett.*, **356**, 298–304.

DiVerdi, J.A. and Opella, S.J. (1982) *J. Am. Chem. Soc.*, **104**, 1761–1762.

Eden, M. and Levitt, M.H. (1999) *J. Chem. Phys.*, **111**, 1511–1519.

Ernst, M. (2003) *J. Magn. Reson.*, **162**, 1–34.

Ernst, M., Samoson, A. and Meier, B.H. (2003) *J. Magn. Reson.*, **163**, 332–339.

Ernst, R.R., Bodenhausen, G. and Wokaun, A. (1987) *Principles of Nuclear Magnetic Resonance in One and Two Dimensions*, Clarendon Press, Oxford.

Gan, Z. and Ernst, R.R. (1997) *Solid State NMR*, **8**, 153–159.

Gerbaud, G., Ziarelli, F. and Caldarelli, S. (2003) *Chem. Phys. Lett.*, **377**, 1–5.

Goetz, J.M. and Schaefer, J. (1997) *J. Magn. Reson.*, **127**, 147–154.

Gullion, T. and Schaefer, J. (1989) *Adv. Magn. Reson.*, **13**, 57–83.

Heise, B., Leppert, J., Ohlenschläger, O., Görlach, M. and Ramachandran, R. (2002) *J. Biomol. NMR*, **24**, 237–243.

Heise, B., Leppert, J., Wenschuh, H., Ohlenschläger, O., Görlach, M. and Ramachandran, R. (2001) *J. Biomol. NMR*, **19**, 167–179.

Hong, M., Gross, J.D. and Griffin, R.G. (1997) *J. Phys. Chem. B*, **101**, 5869–5874.

Hong, M., Gross, J.D., Hu, W. and Griffin, R.G. (1998) *J. Magn. Reson.*, **135**, 169–177.

Hwang, T., van Zijl, P.C.M., and Garwood, M. (1998) *J. Magn. Reson.*, **133**, 200–203.

Kupče, Ē. and Freeman, R. (1995) *J. Magn. Reson. A*, **115**, 273–276.

Kupče, Ē. and Freeman, R. (1996) *Chem. Phys. Lett.*, **250**, 523–527.

Leppert, J., Heise, B., Görlach, M. and Ramachandran, R. (2002) *J. Biomol. NMR*, **23**, 227–238.

Leppert, J., Heise, B., Ohlenschläger, O., Görlach, M. and Ramachandran, R. (2003) *J. Biomol. NMR*, **26**, 13–24.

Leppert, J., Heise, B. and Ramachandran, R. (2000a) *J. Magn. Reson.*, **145**, 307–314.

Leppert, J., Heise, B. and Ramachandran, R. (2000b) *J. Biomol. NMR*, **18**, 153–164.

Leppert, J., Heise, B. and Ramachandran, R. (2001) *Solid State NMR*, **19**, 1–18.

Levitt, M.H., Freeman, R. and Frenkiel, T. (1983) *Adv. Magn. Reson.*, **11**, 47–110.

O'Connor, R.D. and Schaefer, J. (2002) *J. Magn. Reson.*, **154**, 46–52.

Roberts, J.E., Harbison, G.S., Munowitz, M.G., Herzfeld, J. and Griffin, R.G. (1987) *J. Am. Chem. Soc.*, **109**, 4163–4169.

Schmidt-Rohr, K. and Spiess, H.W. (1994) *Multidimensional Solid-State NMR and Polymers*, Academic Press, London.

Shaka, A.J. and Keeler, J. (1987) *Prog. Nucl. Magn. Reson. Spectrosc.*, **19**, 47–129.

Tycko, R., Pines, A. and Guckenheimer, J. (1985) *J. Chem. Phys.*, **83**, 2775–2802.